Supporting Information

Phytate-coordinated nickel foam with enriched NiOOH intermediates for 5-hydroxymethylfurfural electrooxidation

Wangyan Gou,[a#] Yimin Chen,[b#] Yifei Zhong,[c] Qingyu Xue[a], Jiayuan Li[a*] and Yuanyuan Ma[a*]

a Dr. W. Gou, Prof. J. Li, Q. Xue, Prof. Y. Ma,
Key Laboratory of Special Functional and Smart Polymer Materials of Ministry of Industry and Information Technology, School of Chemistry and Chemical Engineering
Northwestern Polytechnical University
Xi'an 710072 (P. R. China)

b Y. Chen
Institute for Frontier Materials
Deakin University
Geelong 3216 (Australia)

c Y. Zhong,
School of Chemical Engineering and Technology
Xi'an Jiaotong University
Xi'an 710049 (P. R. China)

Correspondence and requests for materials should be addressed to Li J. Y. (Email: jiayuanli@nwpu.edu.cn); Ma Y. M. (Email: yyma@nwpu.edu.cn)

This PDF file includes:

Experimental Section

Materials preparation

Chemicals. Hydrochloric acid (HCl, 36.0-38.0 %), acetone (CH_3OCH_3) and ethanol (CH_3CH_2OH) were purchased from Sinopharm Chemical Reagent Co., Ltd. Phytic acid, potassium hydroxide (KOH)5-hydroxymethylfurfural (HMF), 2,5-furandicarboxylic acid (FDCA), 5-hydroxymethyl-2-furan-carboxylic acid (HMFCA), 2,5-diformylfuran (DFF), 2-formyl-5-furancarboxylic acid (FFCA) were obtained from Energy Chemical. Nickel foam (NF) was purchased from Anping Huiruisi Network Co., Ltd. Deionized water with 18.2 $M\Omega \cdot cm^{-1}$ resistance was supplied by a water purification system. All the chemicals were used without further purification.

Synthesis of PA-NF. Firstly, A piece of commercially supplied NF (2×1×0.1 cm^3) was firstly immersed into 1.0 M HCl solution for 15 min and washed with acetone and ethanol to remove surface impurities and oxides. A piece of NF was dipped in the 70 mL aqueous solution containing 3 mL PA for 10 min. Then, the solution was transferred into a 100 mL Teflon-lined stainless-steel autoclave and maintained at 120 °C for 6 h. The as-synthesized electrode was rinsed with water several times, dried at 60 °C in vacuum for 8 h ready for use.

Composition and structure characterization

XRD measurements were conducted on Ultima IV with Cu Kα radiation (λ = 0.1541 nm) from 10° to 90° at 40 kV and 40 mA. The morphology and EDX mapping of samples were analyzed by a ZEISS MERLIN Compact and Oxford x-max operated at an acceleration voltage of 30.0 kV. FT-IR (Thermo Scientific Nicolet iS5) was used to measure the functional group of PA on the NF surface. XPS was measured using a Thermo Scientific K-Alpha equipped with Al Kα monochromatized radiation at 1486.6 eV X-ray source. All binding energies were referenced to the C 1s peak (284.8 eV) arising from the adventitious carbon-containing species. Raman spectra were acquired on an INVIAREFLEX Raman Spectrophotometer with an exciting wavelength of 532 nm. Ni loss was analyzed using a PerkinElmer Optima 2100 DV Inductively coupled plasma mass spectrometer (ICP-MS).

Electrochemical measurements

Electrochemical experiments were conducted on a CHI-760E Electrochemical Workstation (CHI Instruments) typically consisting of a standard three-electrode system. All electrochemical investigations were performed at room temperature using an Ag/AgCl as reference electrode, a graphite rod as counter electrode, and a piece of PA-NF or bare NF served as working electrode, respectively. A 50 mL 1.0 M KOH solution with or without HMF was employed. The measured potentials versus the reversible hydrogen electrode (RHE) were calculated according to Equation (1):

$$E_{RHE} = E_{Ag/AgCl} + 0.197 + 0.059 \times pH \quad (1)$$

All electrochemical reaction was carried out at room temperature (25 ± 1 °C), and the electrolyte was stirred at 800 rpm with a magnetic stir bar. CV measurements were performed at a scan rate of 5 $mV \cdot s^{-1}$. Operando electrochemical impedance spectroscopy (EIS) tests were performed at different applied potentials versus RHE in the frequency range of 0.01-100k Hz by using Autolab PGSTAT302N.

Product analysis

HMF and oxidation products were quantitatively obtained by a HPLC (Waters 1525) equipped with an ultraviolet-visible detector (265 nm) and a 4.6 mm×150 mm Shim-pack GWS 5 μm C 18 column. The mobile phase was HPLC grade methanol and ammonium formate aqueous solution (5 mM, 3:7, flow rate is 0.6 $ml \cdot min^{-1}$). Specifically, 10 μL of electrolyte was removed during potentiostatic electrolysis and diluted to 0.99 ml with ultrapure water. The conversion (%), faradaic efficiency (FE), and yield (%) were calculated based on the Equations (2), (3), and (4), respectively:

$$Conv.\,(\%) = \frac{n(HMF\ consumed)}{n(HMF\ initial)} \times 100 \quad (2)$$

$$Yield.\,(\%) = \frac{n(products\ formed)}{n(HMF\ initial)} \times 100 \quad (3)$$

$$FE\,(\%) = \frac{n(FDCA\ formed)}{charge/(6F)} \times 100 \quad (4)$$

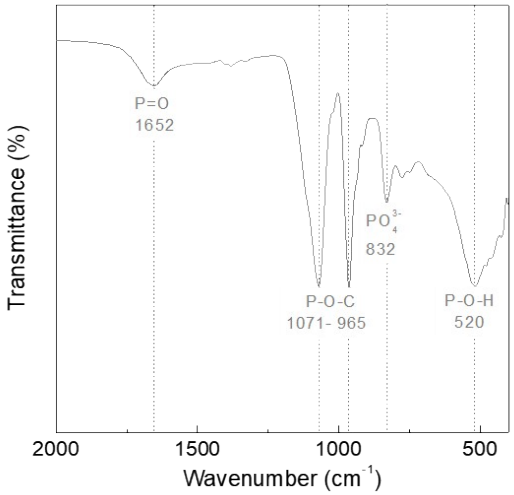

Fig. S1. FT-IR spectrum of phytic acid.

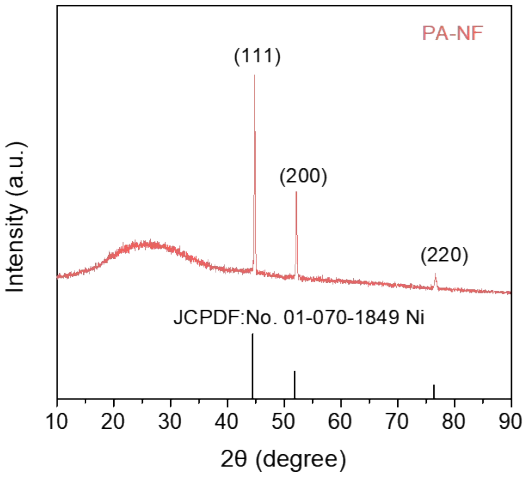

Fig. S2. XRD spectrum of PA-NF.

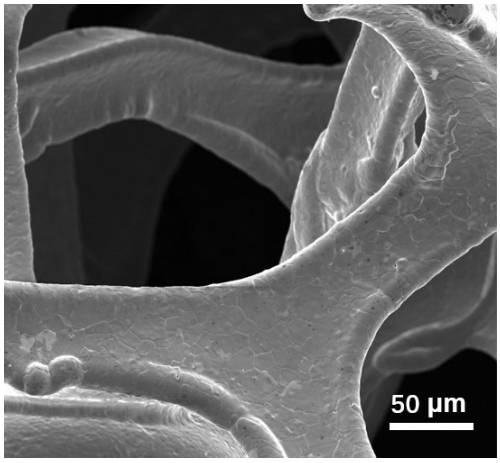

Fig. S3. Low-magnification SEM image of NF.

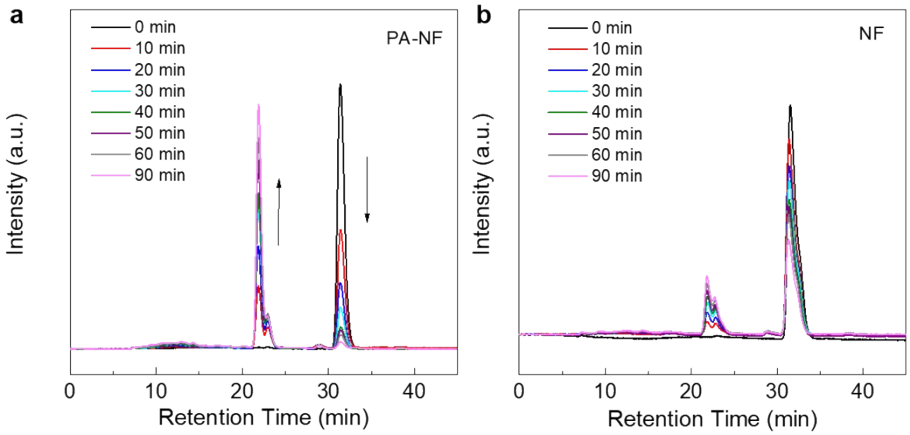

Fig. S4. High performance liquid chromatography analysis results of (a) PA-NF and (b) NF.

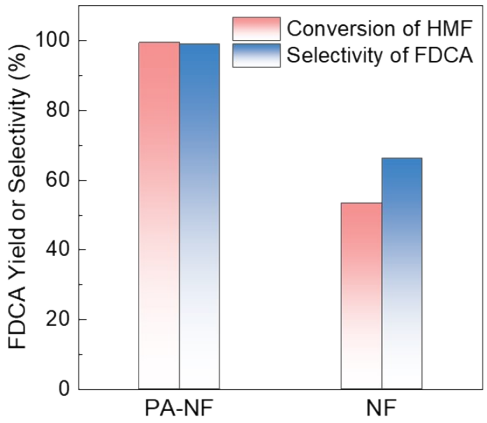

Fig. S5. Conversion of HMF and selectivity of FDCA of PA-NF and NF at 1.40 V_{RHE}.

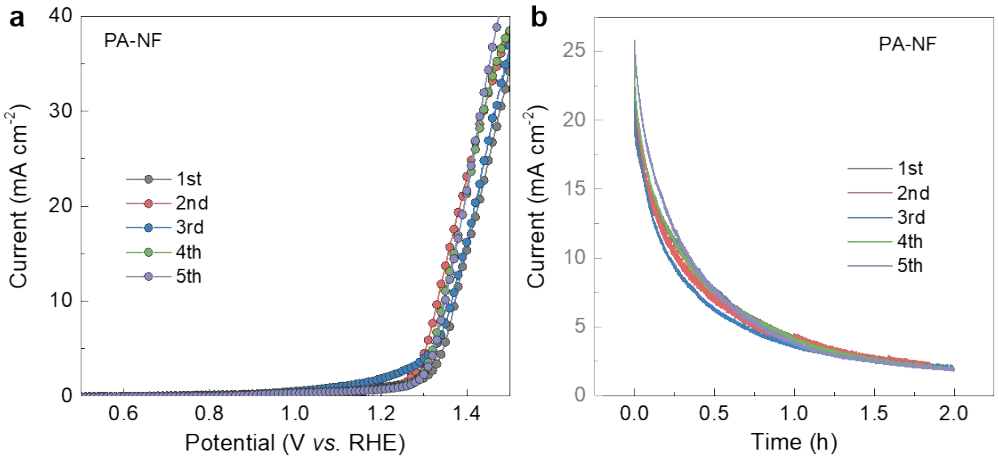

Fig. S6. (a) LSV curves and (b) chronoamperometry curves of PA-NF during five successive reuse cycles.

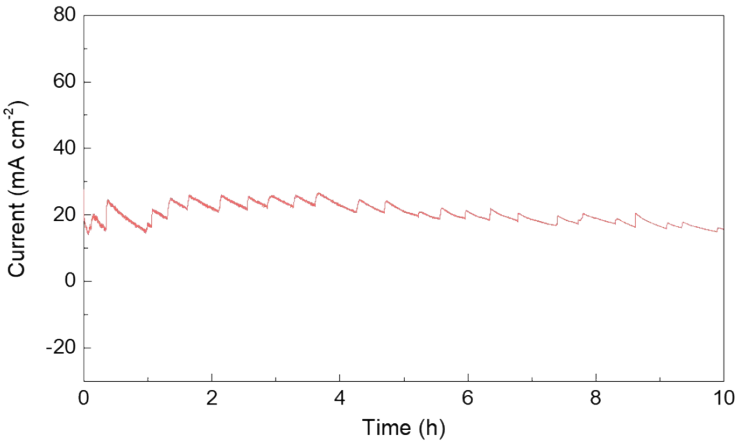

Fig. S7. Catalytic durability over the PA-NF electrode at a constant potential of 1.4 V vs. RHE with continuous supply of HMF.

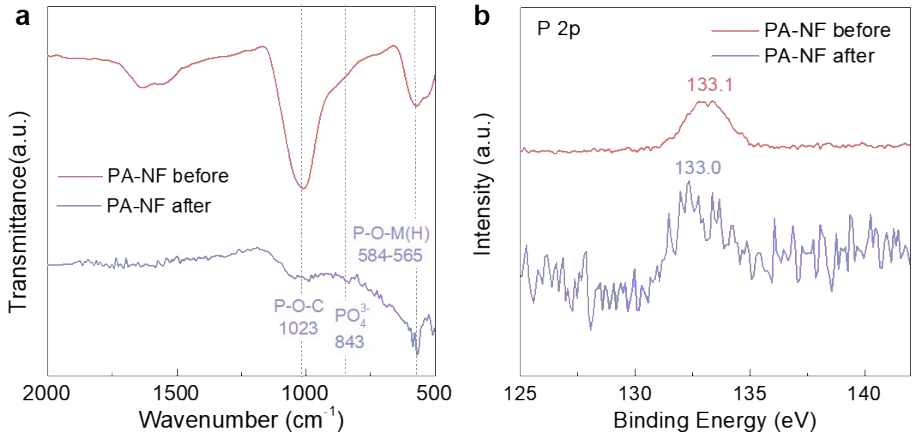

Fig. S8. (a) FT-IR spectra and (b) XPS P 2p spectra of PA-NF before and after HMF electrooxidation, respectively.

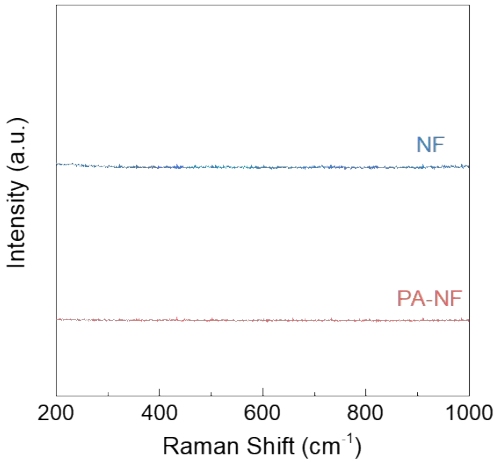

Fig. S9. Raman spectra of PA-NF and NF when HMF were existed in electrolyte.

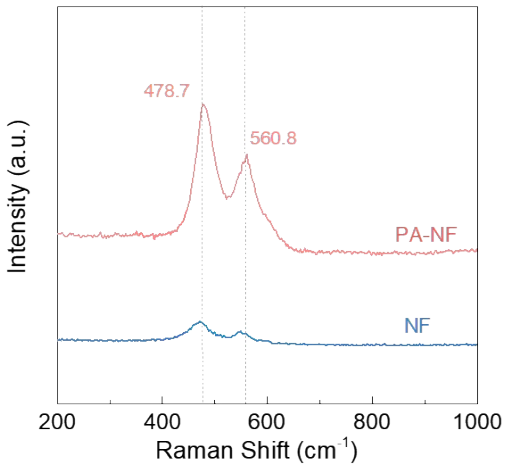

Fig. S10. Raman spectra of PA-NF and NF when HMF were used up in electrolyte.

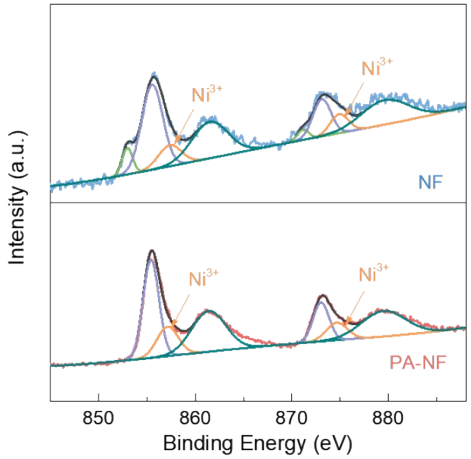

Fig. S11. High-resolution XPS spectra of Ni 2p of PA-NF and NF after HMF electrooxidation reaction.

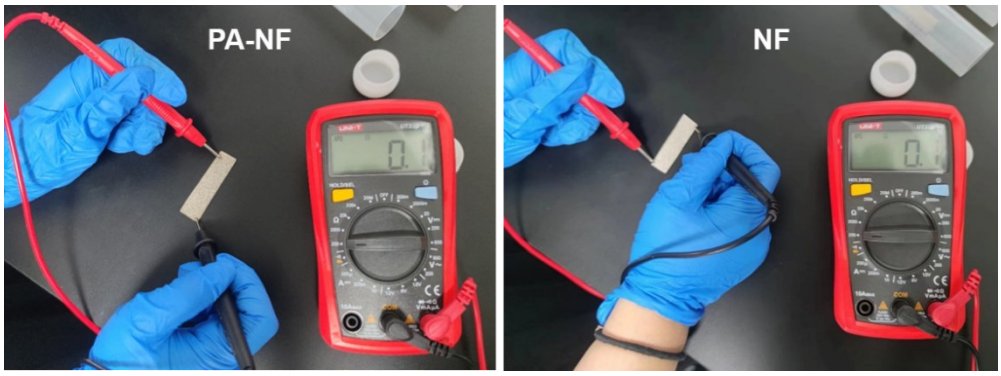

Fig. S12. Condutivity investigations on the PA-NF and NF electrodes.

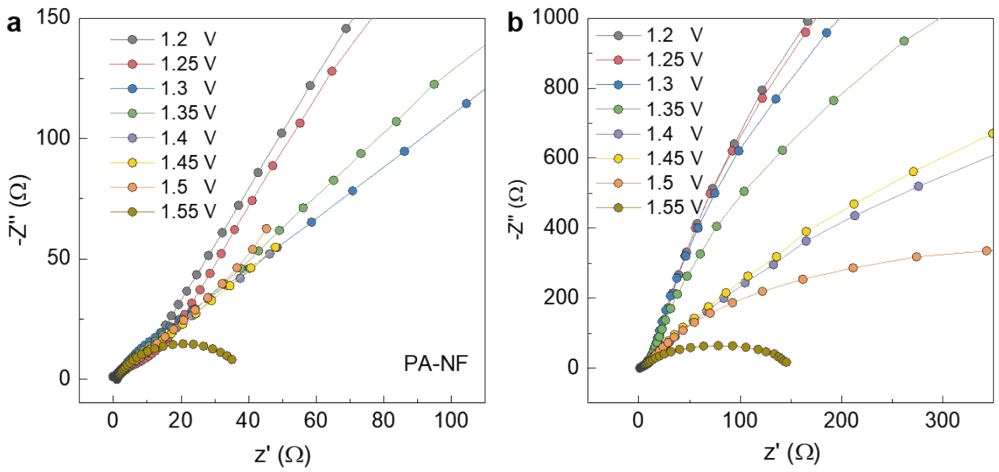

Fig. S13. Nyquist plots of (a) PA-NF and (b) NF electrodes at various potentials in 1 M KOH.

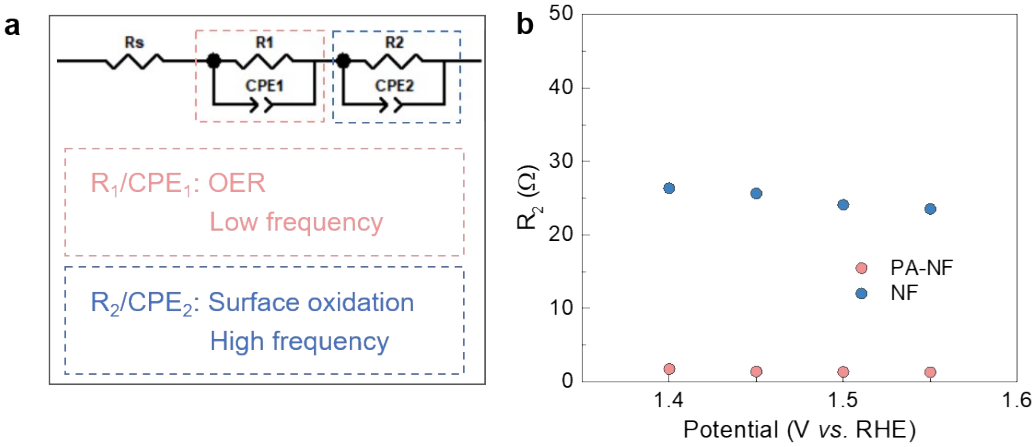

Fig. S14. (a) Equivalent circuit model for Nyquist plots of PA-NF and NF. (b) The fitted R_2 change of PA-NF and NF with applied potential.

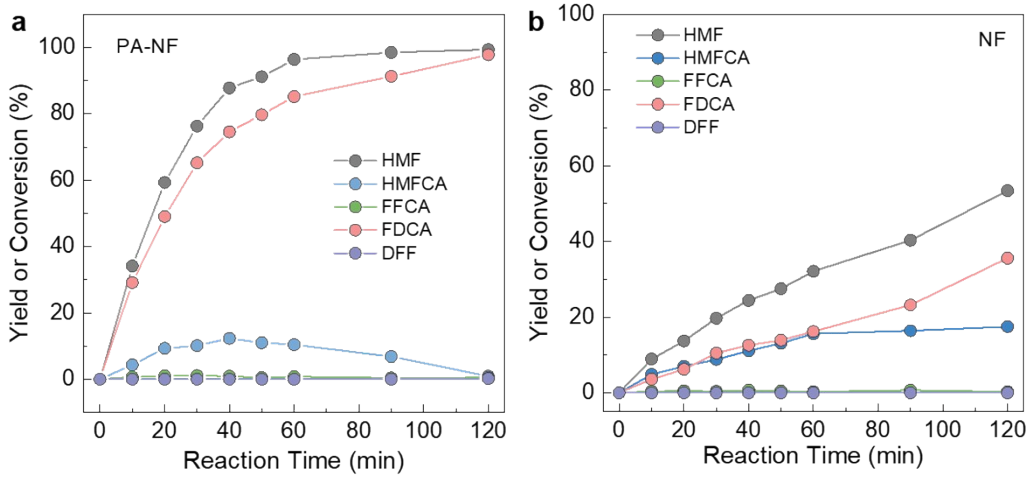

Fig. S15. Conversion of HMF and yield of its oxidation products of (a) PA-NF and (b) NF against reaction time at 1.40 V_{RHE}.

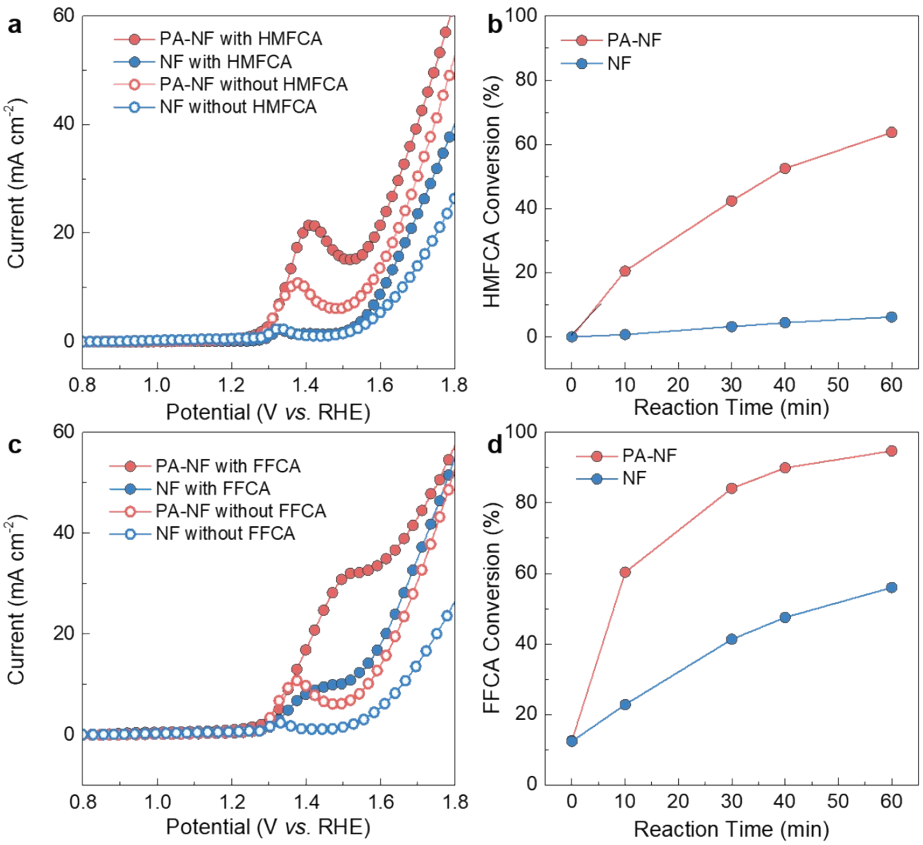

Fig. S16. (a) LSV curves of PA-NF and NF with and without 10 mM HMFCA at a scan rate of 10 $mV \cdot s^{-1}$. (b) Conversion of HMFCA for PA-NF and NF against reaction time at 1.40 V_{RHE}. (c) LSV curves of PA-NF and NF with and without 10 mM FFCA at a scan rate of 10 $mV \cdot s^{-1}$. (d) Conversion of FFCA for PA-NF and NF against reaction time at 1.40 V_{RHE}.

Table S1. Comparison of HMF electrooxidation performance with other non-noble metal catalysts.

Catalyst	Required potential at 20 mA/cm^2 (V vs. RHE)	Conversion of HMF (%)	Selectivity of FDCA (%)	Reaction time (h)	HMF oxidation rate (mmol/h)	Ref.
PA-NF	**1.40**	**99.4**	**98.9%**	**2**	**0.76**	**This work**
NiCoBDC-NF	1.60	88.0	99%	6	0.053	Ref. 1
$NiCo_2O_4$	>1.60	99.6	90.8%	0.9	-	Ref. 2
$CuNi(OH)_2/C$	1.75	>99.9	93.0%	5	0.03	Ref. 3
NiCoFe LDH	1.51	>99.9	84.9%	4	0.32	Ref. 4
Ni(NS)/CC	1.47	99.7	>99.0%	1	0.2	Ref. 5
$Pt/Ni(OH)_2$	1.42	>99.9	98.7%	-	-	Ref. 6
$Ni(OH)_2/NF$	1.33	>99.9	96.0%	1.5	0.35	Ref. 7
$Ni_{0.9}Cu_{0.1}(OH)_2$	1.65	99.7	84%	1.5	-	Ref. 8
$N\text{-}NiMoO_4$	1.43	99.2	97.4%	2	0.14	Ref. 9
NiS_x/Ni_2P	1.346	>99.9	98.5%	2.8	0.16	Ref. 10
Ni_xB-modified	1.42	>99.9	98.5%	0.5	0.27	Ref. 11
$om\text{-}Co_3O_4$	1.45	>99.9	99.8%	-	-	Ref. 12
CoO-CoSe	1.38	>99.9	99.0%	1	-	Ref. 13
MoO_2/FeP	1.38	9.49	98.6%	2.7	0.074	Ref. 14

Table S2. The ICP-MS results of PA-NF after HMF electrooxidation reaction at 1.40 V_{RHE}.

Total electrolyte volume (mL)	Electrolyte volume for ICP-MS (mL)	Measured metal content (ppb)	Mass of leached metal in electrolyte (ug)	Mass of PA-NF (mg)	Ni Loss (%)
50	4	2.9	0.145	56.4	0.00026

Table S3. The fitted parameters of the EIS datas of NF and PA-NF in 1M KOH.

Catalyst	**Potential (V *vs.* RHE)**	**R_S (Ω)**	**n_1**	**R_1 (Ω)**	**$C_{φ1}$ (mF)**	**n_2**	**R_2 (Ω)**	**$C_{φ2}$ (mF)**
PA-NF	1.2	0.93	0.75	12375	1.6	0.81	32.7	1.6
	1.25	0.93	0.73	9538	9.6	0.83	26.6	3.7
	1.3	0.93	0.73	7525	35.9	0.83	15.9	9.6
	1.35	0.93	0.72	4529	61.7	0.81	9.83	31.7
	1.4	0.93	0.72	3717	206.0	0.80	1.74	138.0
	1.45	0.93	0.77	348	264.9	0.81	1.40	140.0
	1.5	0.93	0.76	155	354.9	0.81	1.34	140.0
	1.55	0.93	0.81	38	384.7	0.81	1.31	141.1
NF	1.2	0.96	0.95	25585	8.0	0.82	33.8	2.4
	1.25	0.96	0.96	19610	8.8	0.86	32.61	3.5
	1.3	0.96	0.98	12676	15.8	0.81	31.99	3.8
	1.35	0.96	0.96	7343	24.7	0.83	28.90	6.8
	1.4	0.96	0.91	3934	71.6	0.82	26.34	19.9
	1.45	0.96	0.85	3127	73.9	0.81	25.33	23.2
	1.5	0.96	0.84	865	81.0	0.81	24.10	23.8
	1.55	0.96	0.85	130	83.6	0.85	23.51	22.9

References

1 M. Cai, Y. Zhang, Y. Zhao, Q. Liu, Y. Li and G. Li, *J. Mater. Chem. A*, 2020, **8**, 20386-20392.

2 M. J. Kang, H. Park, J. Jegal, S. Y. Hwang, Y. S. Kang and H. G. Cha, *Appl. Catal. B: Environ.*, 2019, **242**, 85-91.

3 H. Chen, J. Wang, Y. Yao, Z. Zhang, Z. Yang, J. Li, K. Chen, X. Lu, P. Ouyang and J. Fu, *ChemElectroChem*, 2019, **6**, 5797-5801.

4 M. Zhang, Y. Liu, B. Liu, Z. Chen, H. Xu and K. Yan, *ACS Catal.*, 2020, **10**, 5179-5189.

5 X. Lu, K. -H. Wu, B. Zhang, J. Chen, F. Li, B.-J. Su, P. Yan, J.-M. Chen and W. Qi, *Angew. Chem. Int. Ed.*, 2021, **60**, 14528-14535.

6 B. Zhou, Y. Li, Y. Zou, W. Chen, W. Zhou, M. Song, Y. Wu, Y. Lu, J. Liu, Y. Wang and S. Wang, *Angew. Chem. Int. Ed.*, 2021, **60**, 22908-22914.

7 J. Zhang, W. Gong, H. Yin, D. Wang, Y. Zhang, H. Zhang, G. Wang and H. Zhao, *ChemSusChem*, 2021, **14**, 2935-2942.

8 J. Zhang, P. Yu, G. Zeng, F. Bao, Y. Yuan and H. Huang, *J. Mater. Chem. A*, 2021, **9**, 9685-9691.

9 W. Wang and M. Wang, *Catal. Sci. Technol.*, 2021, **11**, 7326-7330.

10 B. Zhang, H. Fu and T. Mu, *Green Chem.*, 2022, **24**, 877-884.

11 S. Barwe, J. Weidner, S. Cychy, D. M. Morales, S. Dieckhöfer, D. Hiltrop, J. Masa, M. Muhler and W. Schuhmann, *Angew. Chem. Int. Ed.*, 2021, **60**, 20535-20542.

12 C. Wang, H. -J. Bongard, M. Yu and F. Schüth, *ChemSusChem*, 2021, **14**, 1-9.

13 X. Huang, J. Song, M. Hua, Z. Xie, S. Liu, T. Wu, G. Yang and B. Han, *Green Chem.*, 2020, **22**, 843-849.

14 G. Yang, Y. Jiao, H. Yan, Y. Xie, A. Wu, X. Dong, D. Guo, C. Tian and H. Fu, *Adv. Mater.*, 2020, **32**, 2000455.